BIOMECHANICS OF BICYCLING

Rory R. Davis
Structural Dynamics Research Corporation
San Diego, California 92111

M. L. Hull
Department of Mechanical Engineering
University of California
Davis, California 95616

ABSTRACT

A computer-based instrumentation system was used to accurately measure the six foot-pedal load components and the absolute pedal position during bicycling. The instrumentation system is the first of its kind and enables extensive and meaningful biomechanical analysis of bicycling. With test subjects "riding" on rollers which simulate actual bicycling, pedalling data were recorded to explore four separate hypotheses. Experiments yielded the following major conclusions: 1) Using cleated shoes retards fatigue of the quadriceps muscle group. By allowing more flexor muscle utilization during the backstroke, cleated shoes distribute the workload and alleviate the peak load demand on the quadriceps group; 2) overall pedalling efficiency increases with power level; 3) non-motive load components which apply adverse moments on the knee joint are of significant magnitude; 4) analysis of pedalling is an invaluable training aid. One test subject reduced his leg exertion at the pedal by 24 percent.

NOMENCLATURE

F_x, F_y, F_z	Force components acting on the bicycle pedal (N)
M_x, M_y, M_z	Moment components acting on the bicycle pedal (Nm)
θ_1	Angle of crank arm relative to vertical (rad)
θ_2	Relative angle between normal to pedal platform and crank arm (rad)
x,y,z	Pedal platform coordinate axes
$\eta(\theta_1)$	Instantaneous motive efficiency
P.I.	Pedalling performance index
F_{max}	Maximum resultant of F_x and F_z (N)
M_{ab}	Resultant magnitude of M_a, M_b (Nm)
M_{xyz}	Total resultant moment magnitude (Nm)

$\pm \theta_x$	Angle of rotation about x axis (rad)
$\pm \theta_z$	Angle of rotation about z axis (rad)
$\pm X$	Translation along x axis (mm)
$T(\theta_1)$	Instantaneous torque (Nm)
P	Average single pedal power level (W)
L_{ca}	Length of the crank arm (mm)

INTRODUCTION

A new bicycling measurement system described by the authors in Part I has enabled extensive pedalling mechanics analysis. The new instrumentation, augmented by the capabilities of specialized computer software for post-processing, was used to investigate several aspects of pedalling. This paper presents the results of those experiments. First, several foot-pedal connection types are investigated to determine their effect on rider fatigue, pedalling power, and efficiency. Second, complete load and pedal angle results are presented and their relation to rider fatigue and overuse injury is discussed. In addition, an attempt is made to develop a set of features that may be used to detect foot orientation changes on the adjustable pedal/dynamometer. This exercise is the first step in the creation of a pattern recognition scheme for detection and prevention of bicycling overuse injuries. Finally, an experiment showing the value of pedalling technique analysis in improving pedalling performance is presented, along with other interesting findings.

Instrumentation and Apparatus

The measurement system consists of four sub-systems: 1) the six component pedal/dynamometer, 2) the pedal position measurement system, 3) signal conditioning electronics, and 4) the minicomputer which digitizes, stores, and analyzes transducer data. The dynamometer, pedal position measurement hardware, and signal conditioning amplifiers were specially designed for this application.

The strain gage pedal/dynamometer incorporating four octagonal rings is shown in Figure 1. All six load components on the pedal are computed from a set of eight independent Wheatstone bridge circuits. Figure 1 also illustrates the potentiometer which measures the relative angle between the pedal and the crank arm. A similar potentiometer is geared to the crank to measure the absolute crank angle. The loads and angles measured are defined in Figure 2. Transducers are designed to fit any commercially available bicycle without modification so that subjects may ride their own bicycles in experiments.

The entire system, including the signal conditioning and digital conversion electronics, is calibrated using a newly developed software routine and a calibration table for precise application of loads to the dynamometer. The potentiometer signals are calibrated automatically during each riding experiment. The calibration techniques are described more fully in Part I.

Data Collection and Analysis

After the measurement system is calibrated, laboratory experiments are performed with the test subjects riding on "rollers" (see Figure 3). Both wheels revolve and no lateral support is provided, so that riders must balance their bicycles just as if they are riding normally. Before riding begins, the data acquisition program measures all static offset voltages of the system. When a test commences the rider pedals against the significant roller friction until the computer operator is satisfied with the speed and steadiness. The computer software operates interactively to continuously write the pedalling speed to the operator. The operator triggers the acquisition program which begins acquiring data at the beginning of the next stroke (pedal top dead center). For most tests, the cycling speed is 8.37 rad/s (80 rpm) and data is taken over three complete revolutions. Data channels are sequentially sampled at 15 kHz in bursts separated by a 1.4 ms interval. Due to sequential sampling, maximum phase error is 2.3×10^{-3} rad (0.16 degrees) which is less than the resolution of the digitized potentiometer signals. The resulting single channel sampling rate is about 500 samples per revolution. The data is stored on hard disk for later processing.

Data analysis is facilitated by special software which performs the following functions automatically:

i) Conditions and calibrates θ_1 and θ_2 data.

ii) Corrects for static offsets and discretizes data further to integral degrees of arc.

iii) Computes the point-by-point average time history of output over three revolutions.

iv) Calculates all applied loads using the previously obtained sensitivity matrix.

v) Calculates instantaneous torque and power applied to the crank.

vi) Calculates motive efficiency as the instantaneous percentage of the total load vector contributing to positive work (the component of load in the direction perpendicular to the crank).

vii) Calculates average power and performance index.

viii) Digitally filters the results to eliminate noise.

ix) Presents results in screen plot form.

In calculating torque, motive efficiency, and average power only loads Fx and Fz are considered. The torque T and motive efficiency η at a point θ_1 degrees into the pedal arc are defined by

$$T(\theta_1) = (Fx \cos \theta_2 - Fz \sin \theta_2) \times L_{ca} \quad (1)$$

$$\eta(\theta_1) = \left(\frac{T(\theta_1)/L_{ca}}{\left[Fx^2 + Fz^2 \right]^{1/2}} \right) \times 100 \text{ percent} \quad (2)$$

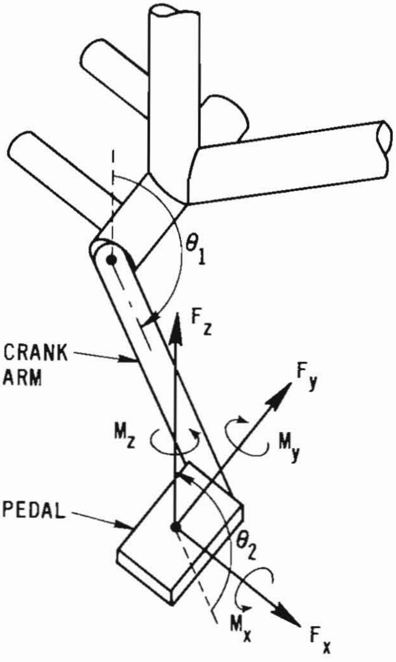

Fig. 2. Definition of dynamometer load components and potentiometer angles.

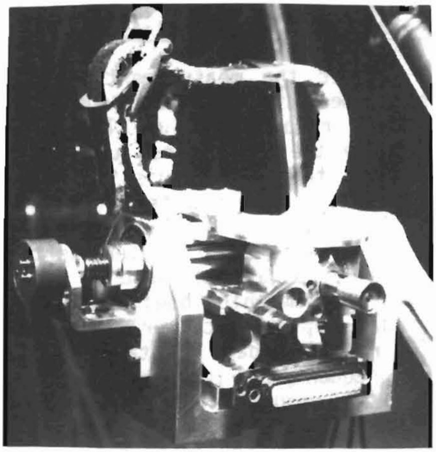

Fig. 1. Six load component pedal/dynamometer.

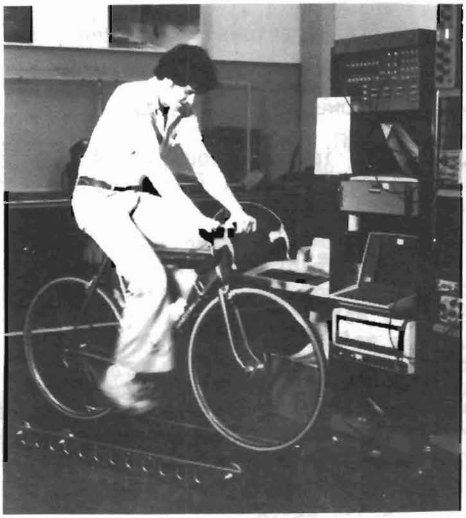

Fig. 3. Riding on rollers in the laboratory.

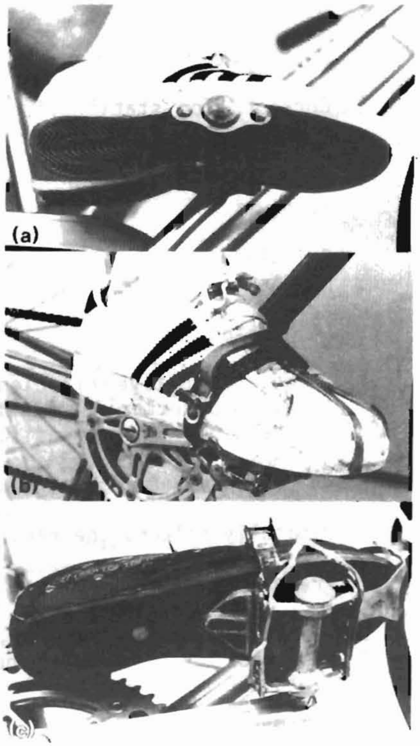

Fig. 4. Three different foot–pedal connections.

where Fx and Fz are functions of θ_1. Note that, as defined, negative efficiencies may result when torque on the crank is negative, against the direction of rotation. Motive efficiency indicates how well a rider utilizes muscle exertion to power the bicycle, while torque presents the magnitude of useful work. Average power P in Watts,

$$\overline{P} = \frac{1}{360}\left(\sum_{\theta_1=1}^{360} T(\theta_1)\ \dot{\theta}_1\right) \tag{3}$$

is also a magnitude measure, convenient for scaling the load histories of one run to another if desired. It must be noted that average power is given only for one leg, and is measured at the point of application of the loads. Since most power measurements were made at the rear wheel in other studies, one must be cautious when comparing results.

A quantitative measure of overall efficiency of converting pedal loads to useful work is given by the performance index. Optimal pedalling force performance would be attained if a rider could apply a maximum constant force perpendicular to the crank arm for a complete cycle. The performance index scales the actual rider to that optimum by the equation

$$\text{P.I.} = \left(\frac{1}{360\ F_{max}} \sum_{\theta_1=1}^{360} T(\theta_1)\right) \times \frac{1}{L_{ca}} \tag{4}$$

where F_{max} is the maximum resultant of Fx and Fz exerted during the cycle. Due to the 360 F_{max} scaling, perfect performance yields a P.I. equal to unity. The P.I. is particularly useful because the normalization allows direct comparison between riders without the need to consider absolute power output.

RESULTS

A. Foot-Pedal Connection Study

Bicycle riders have long realized the relationship between the foot-pedal connection and fatigue and a three-stage foot-pedal connection hierarchy has evolved. In the first stage, force is transferred to a bare pedal through a soft-sole shoe (see Figure 4(a)). Fatigue occurs readily because the only muscle groups active are those which extend the leg. The work of Houtz and Fisher (1959) supports this argument. The next stage adds toeclips to the pedal. Toeclips constrain the longitudinal and transverse position of the shoe as shown in Figure 4(b). Also, a leather strap applies a pre-pressure between the shoe sole and pedal. The toeclips allow more muscle groups to participate in moving the pedals. In the electromyogram studies of Tate and Shierman (1977), data recorded with toeclips showed that flexor muscles were active during the upstroke and the extensor muscles were active over greater arcs. The third stage retains the toeclip but replaces the soft-sole shoe with a special light-weight shoe reinforced with spring steel in the sole (see Figure 4(c)). A cleat fits the pedal so that both longitudinal motion and axial rotation of the foot are prevented. When the toeclip strap is pulled taut the foot cannot be disengaged. From a muscle utilization standpoint, this situation offers clear advantages because more muscles can supply motive power over the pedal arc. Since electromyogram data for the third connection are not in the literature, experiments were performed to document all three connection types and to verify previous findings.

Foot-pedal connection experiments were performed early in the testing program. Data was sampled sequentially at 1000 Hz per channel and only a single revolution was acquired during each run. Several runs under similar conditions verified that major features of the results were repeatable, however. All testing was performed at a pedalling speed of 8.0 rad/s (76 rpm) with a single pedal power level of about 125 W. The rider was an experienced long-distance bicyclist and was not told to pedal in any special manner.

Torque and motive efficiency plots for each of the three foot-pedal connections are shown in Figure 5. Inspection of the results in Figure 5 gives insight into the pedalling process. Several major observations can be made:

i) Use of the cleated shoe greatly improves pedalling efficiency. Note the numerous peaks in efficiency as opposed to the soft shoe results. The additional peak from 190 to 240 degrees indicates an active role of the cleat in power generation. Inspection of load data reveals that larger negative shear loads are produced during the backstroke and the pedal is positioned to utilize that load more effectively. Better plantarflexion control and work by the hamstring muscle group are made possible by the cleat.

ii) In both toeclip cases, additional efficiency is achieved early in the pedalling cycle during the first 25 degrees of arc. This is primarily due to greater dorsiflexion which enhances normal load utilization. Additionally, the toeclip provides greater shear (Fx) capability.

iii) The maximum torque level decreases with the addition of toeclips and cleats. For the shoe sans toeclip, negative torques exist over 160 degrees of pedal arc and the energy lost must be regained by increasing normal pedal load (and torque) in the first half of the cycle. When the toeclips are added, improved efficiency early in the cycle lessens the dependence on extensor muscles to provide the major motive work, despite the less severe, but still present negative torques occurring in the backstroke.

iv) Torque history changes dramatically with the addition of cleats. Maximum torque is lower since efficiency in the backstroke couples with significant negative shear load to produce positive torque past 200 degrees of arc. In fact, negative torque occurs only for 55 degrees of arc with the cleated shoe. Clearly, the cleats allow enhanced activity of the flexor muscle groups.

Initial testing showed that fewer data points per revolution were adequate to accurately describe the loads. Therefore, the sampling algorithm was altered to sample at a slower rate while maintaining small phase error with the "burst" sampling technique described earlier. The remainder of the tests were performed with the right pedal instrumented and the slower sampling enabled acquisition of 3 complete cycles which were point-by-point averaged during post-processing. Toeclips and cleats were used by the riders and all data were taken at 8.37 rad/s (80 rpm).

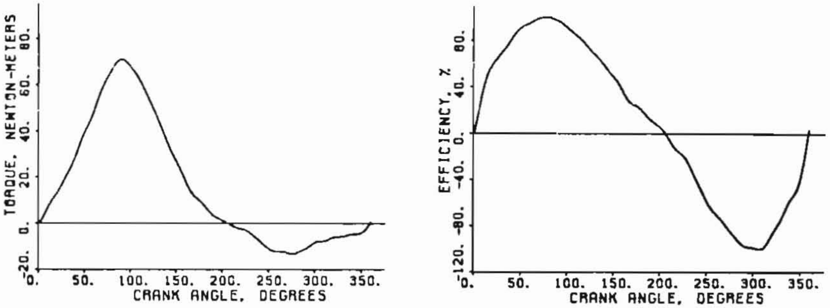

(a) soft sole shoe

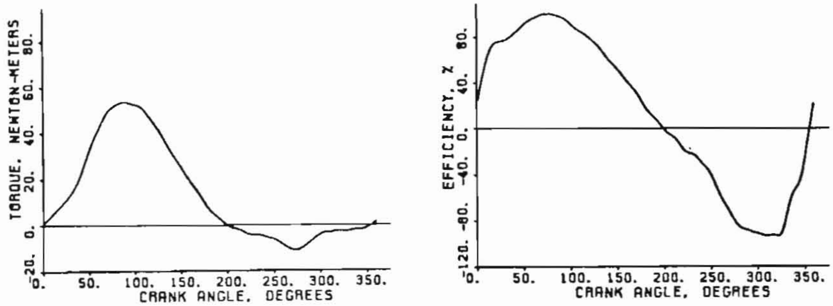

(b) soft sole shoe with toeclip

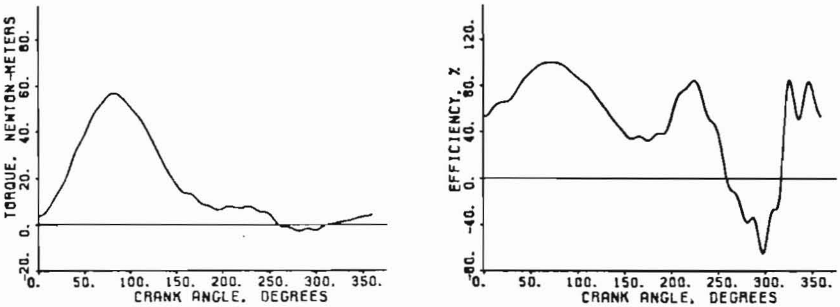

(c) lightweight shoe with cleat and toeclip

Figure 5. Torque and motive efficiency for the three foot-pedal connections at a single pedal power level of 125 W and 8.0 rad/s (76 rpm)

A number of riders performed in the tests that follow. Briefly, they can be described as:

Rider A: Experienced amateur racer, places well in long-distance races, Male.

Rider B: Alternate for U.S. Junior National Team, Male.

Rider C: One of the top female racers in the U.S.

Rider D: Inexperienced bicyclist, Male.

Rider E: Experienced long-distance bicyclist (was subject for foot-pedal connection study), Male.

Rider F: Experienced long-distance bicyclist, Male.

B. General Pedal Load Results

Figure 6 presents the complete load profiles for rider A with a single pedal power level of 180 W. The general features of a typical load profile are contained in Figure 6 and will be discussed. Figure 7 contains the pedal angle, torque, and efficiency plots for the same run. The most prominent feature of the load profiles is the shape of the normal load (Fz) curve. As in Figure 6(a), the load reaches a maximum magnitude in the range of 90 to 110 degrees and then the magnitude decreases toward zero. The two maxima during the backstroke (180-360 degrees) almost always occur and excursions above zero of significant magnitude are rare. The dip between maxima always occurs near 270 degrees, where the horizontal velocity of the foot changes direction. Therefore, the dip may be due to inertial loads.

Another notable feature of the loading is that Fy and Mz are always in phase with the normal load Fz. They all reach maximum magnitudes at about the same point. As the rider pushes downward in the maximum load zone of the stroke, the foot also pushes outward on the pedal and the heel of the foot tends to twist outward. The twist is a simple result of the moment caused by noncoincidence of the point of application of Fy and the central axis of the lower leg. The origin of Fy is not as easily ascertained but is likely to be caused by the geometry of the human body relative to the pedals. Since the magnitudes of Fy and Mz are significant (Fy is usually of the same order as the driving force Fx), and since both exert adverse moments on the knee joint, measures to decrease or eliminate these loads may be beneficial. It is of utmost importance from an injury standpoint that Fy and Mz are not negligible, as usually assumed in bicycling analyses.

The profile of the force Fx in Figure 6(c) is a typical one when cleats with toeclips are used. Positive shear (forward) occurs during the first part of the stroke. As the pedal moves downward, the shear load shifts to a negative value to maintain a positive torque contribution. It is interesting to note that the negative of the Fx profile nearly matches the My profile. It may seem surprising that My is not always zero because the pedal platform is fixed to the spindle with low friction ball bearings. The development of such a moment is made possible by the interaction of the shoe, pedal, and toeclip. The My moment is a necessary byproduct of the shear force Fx because the total moment about the pedal spindle must be nearly zero.

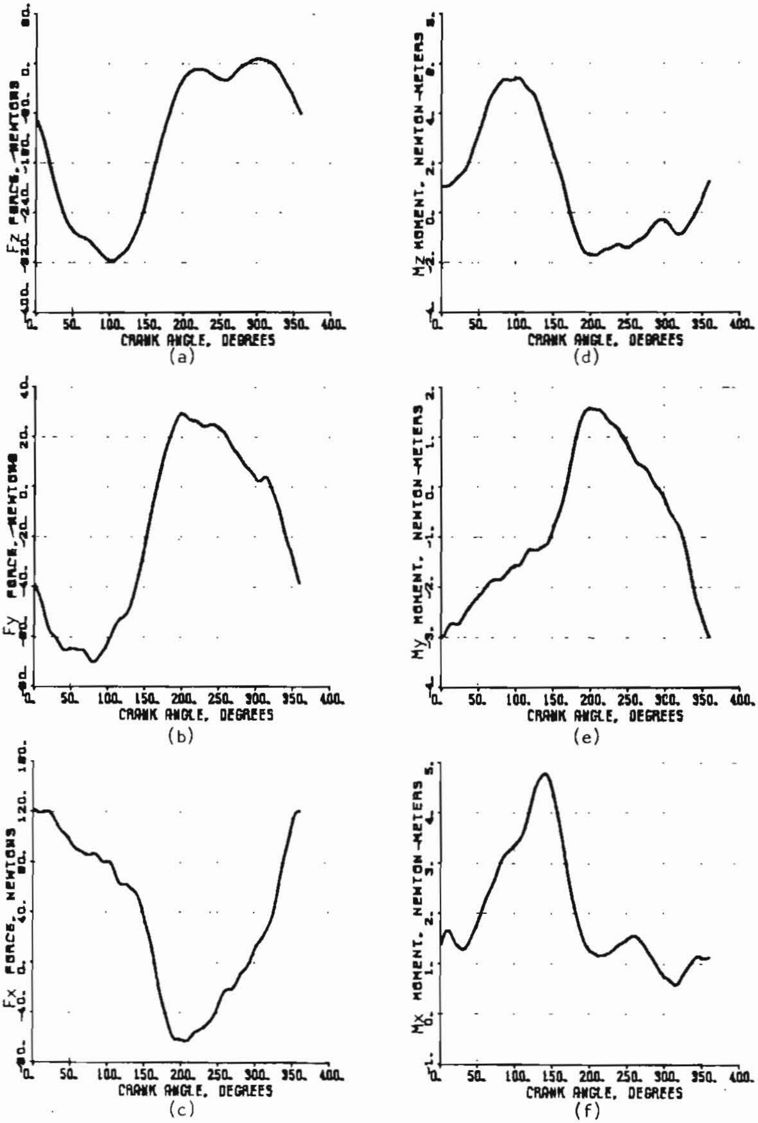

Fig. 6. Typical pedal loading of rider A at 180W single pedal power level and 80 rpm.

Accordingly, resolving Fx and My about the pedal spindle axis yields almost zero moment at that point. Any small non-zero remainder is due to friction in the bearings and rotary inertial load of the pedal itself.

The most unpredictable load component is the moment Mx. Mx is generated whenever the point of application of Fz moves laterally from the center of the pedal. Such motion depends on several highly variable factors, such as lateral constraint of the foot and condition of the shoe cleat grooves. Therefore, large variations of Mx profiles are observed among riders. From an injury perspective, Mx is relatively unimportant. For example, the moment caused by Fy on the knee in the same direction as Mx is a maximum of 36 Nm for rider A, seven times the maximum value of Mx.

Several other details of the interaction between the different outputs merit discussion. Most importantly, note that efficiency reaches 100 percent before the normal load Fz reaches its maximum magnitude (see Figures 6 and 7). At a crank angle of 75 degrees, the pedal platform is nearly horizontal, not parallel to the crank arm. Due to the positive shear load, however, the resultant load is perpendicular to the crank and, hence, 100 percent efficiency is achieved. Since the maximum resultant load occurs some time after 75 degrees when efficiency is sub-optimal, rider A has wasted some of the maximum load available.

A second point of interest occurs at a crank angle of approximately 220 degrees where the efficiency curve exhibits a second peak. High efficiency occurs because the pedal platform is nearly perpendicular to the crank arm and the shear force Fx is twice the normal force Fz. During the upstroke, the majority of torque is produced by inclining the pedal and pulling back rather than pulling vertically up on the pedal through the leather strap.

One feature of Figure 7, which is not consistent among all riders, is the high efficiency profile. In comparing Figure 7 to Figure 5, also note that rider A managed to maintain positive torque for the entire cycle. It has been found that such performance is achieved by subtle changes in pedal angle and load profiles.

The preceding discussion indicates the importance of proper pedal orientation in achieving high pedalling efficiency. Importance of pedal orientation is well known by competitive cyclists who employ a process called ankling to control pedal position. Mastery of the technique, however, is not a simple process since riders normally have no direct method of performance evaluation available. As a result, overall pedalling efficiency varies widely among riders. Table 1 presents the best performance index for each of the riders during the main testing sequence. Note that riders E and F have similar riding experience and rode the same bicycle during tests at similar power levels, but the P.I. levels are different by about 15 percent. Furthermore, rider A's P.I. is 15 percent to 20 percent greater than rider E's, although the same bicycle was again used. Riders B and C, using their own bicycles, yielded low P.I. values despite their extensive riding experience. This contradiction may be a result of the low power level for their tests relative to the others.

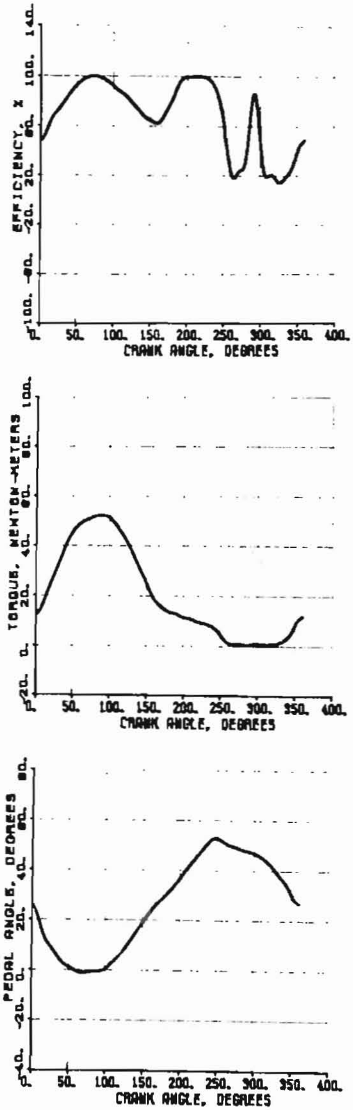

Fig. 7. Companion torque, motive efficiency and pedal angle for rider A.

TABLE 1. Best performance indices achieved by test subjects at 8.37 rad/s (80 rpm)

Rider	Power Level*, W	Performance Index
A+	180	0.370
B	110	0.260
C	100	0.260
D	200	0.289
E	175	0.308
F	160	0.259

* Single pedal

+ This was achieved during the run shown in Figures 6 and 7.

Further evidence suggests a relationship between power level and performance index. Examining the test results of the inexperienced rider D shows that the P.I. is greater than that of three of the more experienced riders. The high power level may be a factor in this case since rider D maintained a power level about twice as great as riders B and C. Power level differences were due to bicycle tire pressure and type, lubrication, and drive ratio.

C. Power Level Effects on Efficiency

Rider D was chosen for these tests because a more experienced rider would probably utilize special ankling techniques at the higher loads. The objective was to observe whether efficiency improvement occurs naturally with greater power level.

The results of tests at three different power levels are superimposed in Figures 8 and 9. Power level was varied using the bicycle's gears, while holding cranking speed constant. Note that as power level increases, efficiency in the 180 to 300 degree range improves significantly. The performance index gradually increases from 0.215 for the 85 W test to 0.266 and 0.289 for the 140 and 200 W tests, respectively. Therefore, increasing power output by a factor of 2.4 requires only a factor of 1.8 increase in leg exertion at the pedal.

In light of the finding above, it may appear that a rider could extend bicycling range by riding at a higher power level. However, the resistances to motion during actual bicycling must be considered. Air drag force, the major deterrent in bicycling, varies with the square of the speed, and hence power varies with the cube (see Whitt and Wilson (1974)). Therefore, the

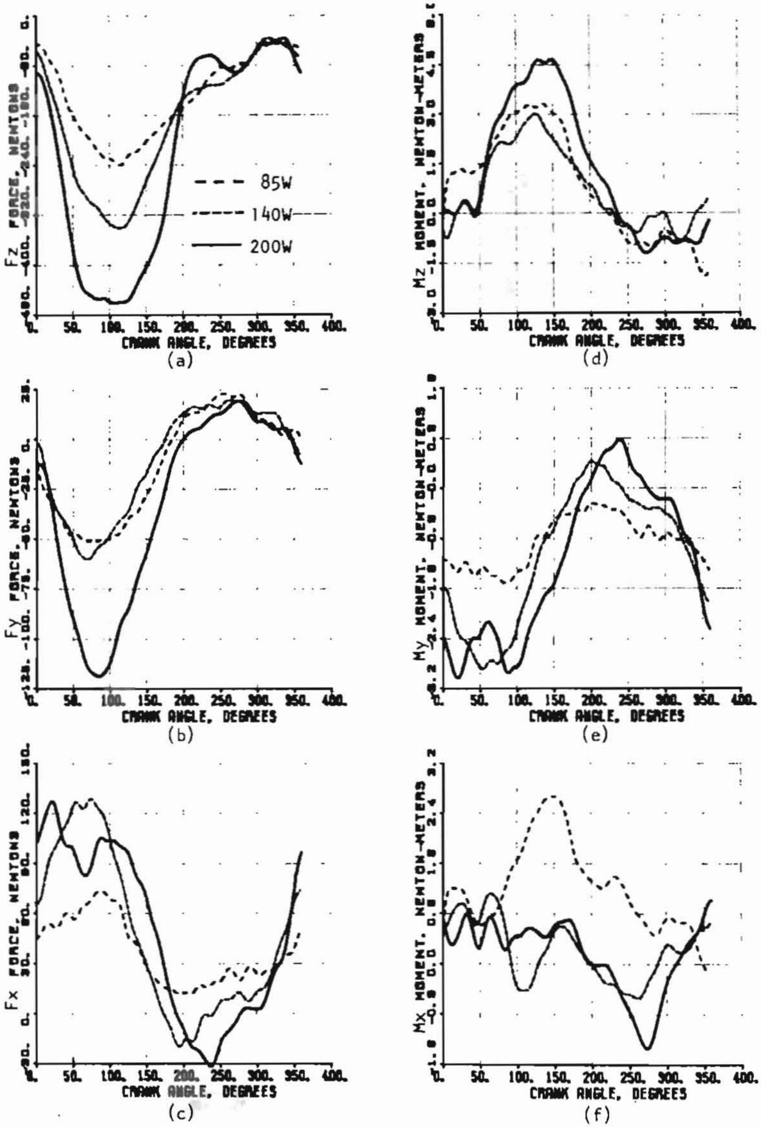

Fig. 8. Load profiles of rider D at three different power levels

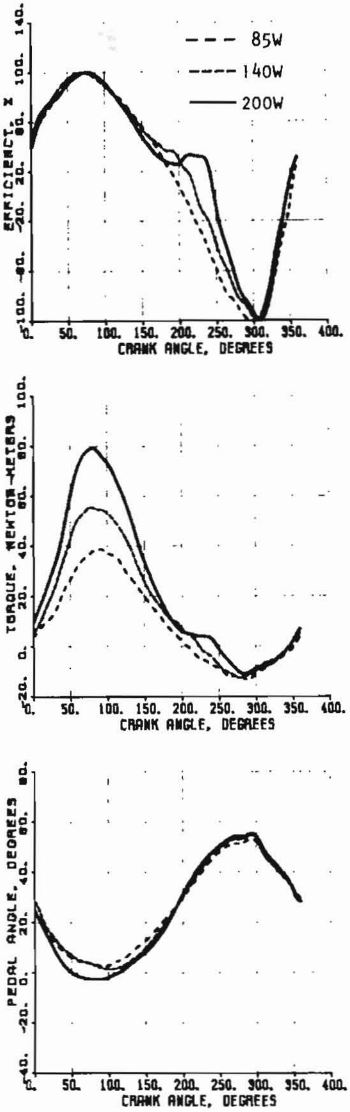

Fig. 9. Companion torque, motive efficiency and pedal angle for rider D at three different power levels

factor of 2.4 increase in power would result in a factor of 1.34 increase in road speed. Since the force exertion factor is greater than the speed factor, total range is decreased assuming a fixed amount of energy is available to the rider. The situation is analogous to an automobile, where fuel consumption increases disproportionately with speed; although in the bicyclist's case, the power plant efficiency (performance index) increases with power level.

The cause of the increase in P.I. for higher power levels may be deduced by inspecting the profiles. Pedal angle changes little during the backstroke but the magnitudes of Fx and Fz are quite different for each test. Negative shear in the backstroke increases significantly and the backstroke maxima of the normal force become more pronounced. Note the lobe in Fz developed during the 200 W test near 230 degrees. Although the lobe never exceeds zero, the benefits of less negative torque due to normal load are reflected by higher efficiencies. The torque plot shows negative torque occuring over about 100 degrees of arc instead of 140 degrees as in the 85 W test.

Figure 8(f) shows that the Mx moment is indeed quite random, even between tests with the same rider. Accordingly, the moment appears to be primarily due to inadequate lateral foot constraint by the leather strap. The Fy and Mz plots also show some interesting behavior. Although both loads track the normal load Fz in phase, the magnitudes are not related to Fz in any simple manner. Finally, the similarity between Fz and the torque shows that the majority of power increase is provided by greater normal load (extensor activity) during the downstroke.

D. Pedal Orientation Experiments

Extensive testing was performed with riders A, B, C, E and F to investigate the effect of foot orientation on load history. Each rider performed a minimum of 7 tests which included positive and negative adjustments in three directions and a normal adjustment test for comparison. Specifically, adjustments included ± 3 degrees rotation in the z-direction ($\pm \theta_Z$), ± 5 degrees rotation in the x-direction ($\pm \theta_X$), and ± 0.5 cm translation in the x-direction relative to the pedal spindle (± X).

Figure 10 presents the load profiles of rider A for the normal test with results for positive and negative adjustment of θ_Z superimposed. Although changes in the load profiles of Figure 10 are not large, there do appear to be some features of the loading that distinguish one adjustment from the other. For example, the value of Mz increases or decreases during the second half of the stroke depending on whether the adjustment is negative or positive, respectively. Other features concerned with peak or range magnitudes may be selected which yield meaningful distinctions between adjustments.

It should be noted that Figure 10 is presented as an example but is not typical of tests with other riders. It was found that, in most cases, visibly useful features extracted from one rider's results were contradicted by the results of some or all of the remaining rider tests. Additional computer software was therefore developed in an effort to identify representative features not discernible by visual inspection.

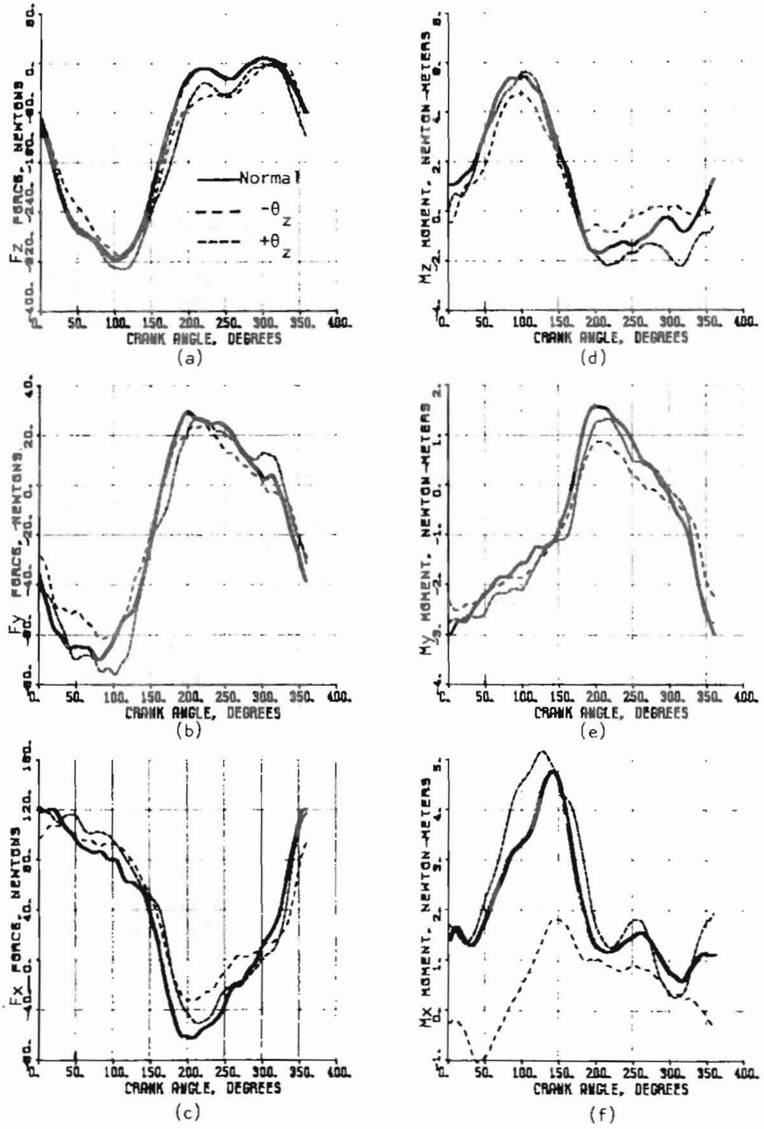

Fig. 10. Load profiles of rider A for three axial foot rotation adjustments

The three moment components were affected most by foot orientation adjustments, so subsequent feature calculations were performed on Mx, My and Mz only. First, average and RMS (root mean square) values of the moments were calculated for three intervals of pedal arc: zero to 180 degrees, 180 to 360 degrees, and full cycle. In addition, all permutations of resultant magnitudes of the moments (e.g. $(Mx^2 + My^2)^{1/2} = Mxy$, etc.) were calculated as functions of pedal arc. Finally, the resultants were processed to yield their average and RMS values over the three intervals discussed.

Unfortunately, the calculations failed to identify any loading features representative of all riders for a particular foot-pedal adjustment. However, some features were found to be common among groups of two or three riders who were tested at similar power levels. For example, the RMS value of the total moment resultant (Mxyz) over the second half of pedal arc was found to be a diagnostic feature for θ_z adjustment for riders A, E, and F. These three riders were tested at similar power levels as Table 1 indicates.

While several features were identified as diagnostic for subsets of riders, assembly of enough independent features to separately identify the adjustments was not possible in this investigation.

E. Performance Briefing Experiment

As discussed earlier, results of bicycling tests showed that pedalling performance index varied greatly among the riders and the P.I. did not appear to hold any correspondence with cyclist experience. Both riders and investigators hypothesized, however, that pedalling efficiency and hence P.I. could be improved, especially when the appropriate feedback was returned to the rider. Therefore a simple experiment was performed to investigate the effect that discussion of pedalling technique has on rider performance.

In initial phases of testing before any discussions, rider E had performed several runs at a power level of 160 W. One typical run was used as a control case and rider E became the subject of the experiment. Before subsequent testing, rider E was briefed concerning his pedalling technique with the use of the solid line control case data in Figure 11 (denoted "before"). The most prominent flaw in the cycle was the occurrence of negative torque during the backstroke. To remedy the situation, rider E was instructed to increase both normal pull and negative shear on the pedal during the backstroke. Since the shear load was larger than the normal load in the original test, rider E was also advised to use greater "ankling" to better utilize the shear load in the 200 to 270 degree range (calf muscle contraction). All these modifications would help raise the efficiency curve (see Figure 11(d)) in the latter stages of the cycle. A final recommendation was made to shift the main peak in efficiency to correspond with the peak in Fz magnitude. Although this modification would not increase efficiency, it would induce larger terms in the numerator of the P.I. expression (Eq. (4)). Calculations showed that the efficiency shift could be achieved by altering "ankling" behavior to extend the toe earlier in the stroke.

The dashed line data in Figure 11 shows the results of a test of rider E at the same power level after briefing. The improvement in backstroke efficiency is dramatic and the resulting torque output remains positive over the entire cycle. While pedal angle shows improved calf activity in the 200

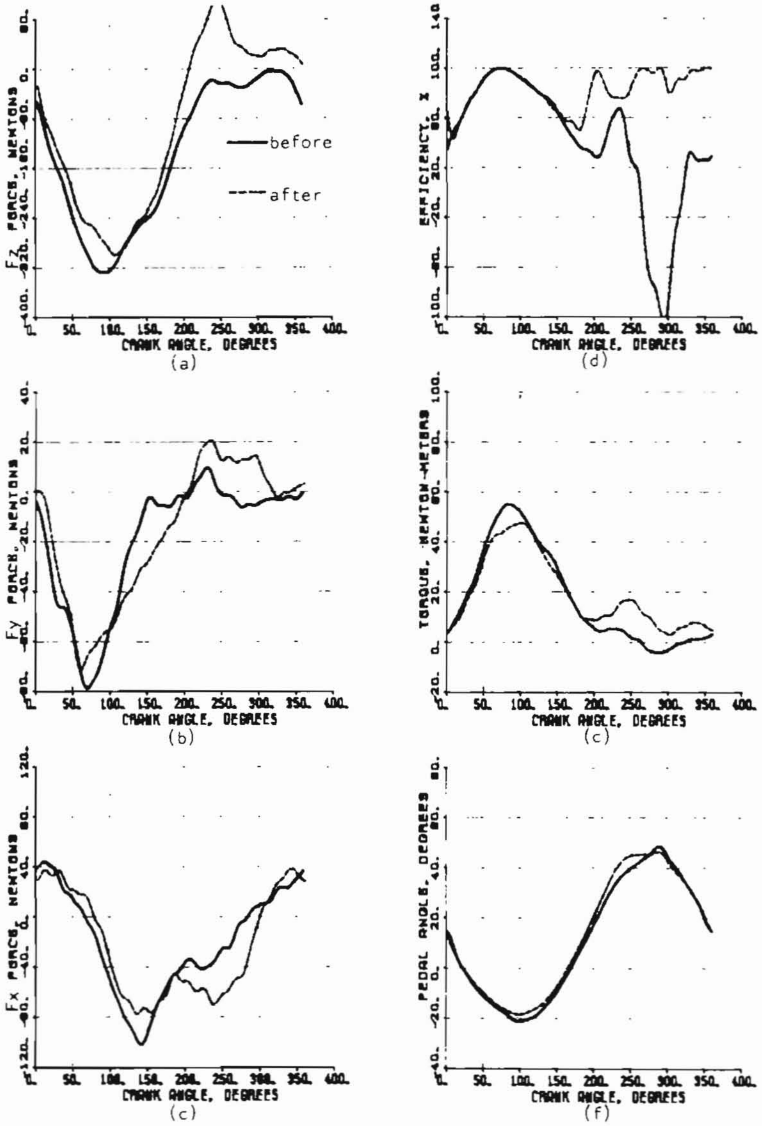

Fig. 11. Pedal force and other results before and after pedalling technique analysis of rider E.

to 270 degree range, the vast majority of added efficiency and torque is due to altered load profiles. Rider pull on the pedal is quite pronounced in Figure 11(a), where Fz remains positive for over 40 percent of the total pedal arc. Such a result is unprecedented in the literature concerning bicycling measurement. The much greater positive normal load tends to align the total load vector more perpendicular to the crank arm and hence increases efficiency. In addition, Fx shows larger magnitudes in the 200 to 300 degree range, which translates into higher torque in the backstroke.

A convenient by-product of the improved backstroke performance is the decrease of peak magnitudes of all the force components. Constancy of the power level requires that total area under the torque curve remain constant assuming no variation in angular velocity. The increase in torque from 200 to 350 degrees caused by enhanced flexor muscle activity relieves the load necessary from extensor groups in the 50 to 100 degree range of maximum exertion. The improvements gained by briefing raised the P.I. value from 0.29 to 0.38, which translates to a savings in rider leg exertion at the pedal of 24 percent.

CONCLUSIONS

The results presented here both confirm the conclusions of previous research and shed new light on the pedalling process. The results of the foot-pedal connection study support the findings of Houtz and Fisher (1959). Also, Tate and Shierman's (1977) claim that more muscle groups come into play with toe-clips is substantiated. However, toeclips alone do not produce an increase in the amount of pedal arc that experiences positive work. The primary function of the toeclip is to increase efficiency by permitting greater dorsiflexion and shear loads in the initial stages of the pedalling cycle.

Additionally, it was found that cleats allow a marked increase in flexor muscle activity, especially during the backstroke. Contrary to popular belief, negative shear load rather than positive normal load is most important during the backstroke. The normal load is almost always contributing negatively to the torque during this phase. By producing the highest pedalling efficiency and alleviating the extensor muscle loads, cleats appear to help decrease lower extremity muscle fatigue in bicycling.

General attributes of load profiles were found to be similar among riders (except Mx), and greater efficiency was achieved by subtle changes in the Fx, Fz and pedal angle profiles that appeared to cost little in terms of rider energy expenditure. The magnitudes of Fy and Mz were found to be significant and measures to eliminate those adverse loads will probably be beneficial in alleviating rider knee injury. Rider injury and fatigue are likely to be minimized by modifying pedalling technique to more evenly distribute muscle requirements throughout the lower extremity.

The significance of performance index in relation to rider fatigue merits additional discussion. It should be noted that in the strictest sense, P.I. measures the rider's overall ability to convert pedal loads to useful work during pedalling. Therefore, the P.I. does not directly involve the actual rider muscle exertion, only the end result of muscle exertion (load at the pedal). However, the following observations lead to the conclusion that P.I. can also indicate the actual muscle exertion of the rider:

1) P.I. can be increased greatly by a relatively small variation in pedalling technique. The muscle energy cost of varying the technique is therefore small, while the greater P.I. enables significantly enhanced power output for comparable load magnitudes. In other words, the main effect is the shifting of existing loads to more useful orientations. Therefore, neither muscle exertion nor load magnitude are greatly affected.

2) The pedal load components important for torque, efficiency, and P.I. calculations are closely related to the action of the larger leg muscle groups (e.g. flexors and extensors). It would therefore be reasonable to assume that the pedal load components are good indicators of overall leg muscle exertion.

3) Some leg muscle work is not reflected in the pedal load data and subsequent calculations. For example, the energy cost of lifting the leg against gravity (when one tries to pull up on the pedal in the backstroke to improve efficiency) is not considered in the P.I. However, these types of exertions are small in comparison to the main leg muscle action. Consequently, assuming that P.I. indicates muscle exertion is reasonable.

Although the use of the P.I. for overall muscle exertion study is only approximate, it is felt to be of practical utility in pedalling performance evaluation. An increase in P.I. at a specific power level will most likely give a decrease in muscle exertion. Further study on the relationship between performance index and rider exertion is warranted, however.

Performance index was found to vary appreciably among riders and results show that pedalling technique is a complex subject not easily understood and mastered by even experienced riders without advanced assistance. It appears that successful cycling is presently predicated upon development of stamina and strength with a lesser emphasis on pedallng technique and efficiency.

Overall pedalling force-to-torque conversion (P.I.) was found to naturally increase with power level but air drag effects in bicycling preclude the ability to extend cycling range by increasing speed (and power level).

Pedal orientation testing and analysis failed to produce the features necessary to accurately diagnose foot orientation adjustment. However, some features were found to be diagnostic when power level was common among the tests. Therefore, additional analytical and experimental research may unearth the features needed to complete the classifier. The problem is complex and warrants more intensive study.

The specialized measurement and analysis system utilized proved to be an easily used, extremely valuable tool for bicycling mechanics analysis. Advanced analysis capabilities enable the timely output of accurate and useful data such as torque and efficiency profiles, and most importantly, performance index which condenses a complex set of outputs into a single pedalling technique measure. The utility of such output data was proven by the outcome of the performance briefing experiment, where a simple discussion of technique resulted in a 24 percent savings in rider leg exertion at the pedal. The possibilities for rider training to improve energy utilization and minimize fatigue are very promising.

ACKNOWLEDGEMENTS

The authors are indebted to the University of California for it's support. We thank Mr. John Ramming for his advice and assistance during the calibration and software development phases of the project. Finally, we are grateful to Ms. Lesa Havert who very ably prepared the manuscript.

REFERENCES

Houtz, S.F., and Fisher, F.J., (1959) "An Analysis of Muscle Action and Joint Excursion on a Stationary Bicycle," The Journal of Bone and Joint Surgery, Vol. 41-A, No. 1, pp. 123-131.

Hull, M.L. and Davis, R.R., (1981) "Measurement of Pedal Loading During Bicycling: I. Instrumentation," Journal of Biomechanics, Vol. 14, No. 12, pp. 843-855.

Tate, J. and Shierman, G., (1977) "Toe Clips: How They Increase Pedalling Efficiency," Bicycling, Vol. 18, No. 6, p. 57.

Whitt, F.R. and Wilson, D.G., (1974) Bicycling Science, MIT Press, Cambridge.